

Impact of PDF uncertainties at large x on heavy boson production

L. T. Brady^{1,2}, A. Accardi^{1,3}, W. Melnitchouk¹, J. F. Owens⁴

¹*Jefferson Lab, Newport News, Virginia 23606*

²*Harvey Mudd College, Claremont, California 91711*

³*Hampton University, Hampton, Virginia 23668*

⁴*Florida State University, Tallahassee, Florida 32306*

Abstract

We explore the sensitivity of W and Z boson production in hadronic collisions to uncertainties in parton distribution functions (PDFs) at large x arising from uncertainties in nuclear corrections when using deuterium data in global QCD fits. The W and Z differential cross sections show increasing influence of nuclear corrections at high boson rapidities, particularly for the d quark, which is diluted somewhat in the decay lepton rapidity distributions. The effects of PDF uncertainties on heavy W' and Z' bosons beyond the Standard Model become progressively more important for larger boson masses or rapidities, both in pp collisions at the LHC and in $p\bar{p}$ scattering at the Tevatron.

I. INTRODUCTION

The discovery and determination of properties of new particles beyond the Standard Model at high-energy colliders depends on accurate knowledge of parton distribution functions (PDFs) of the hadrons involved in the collisions. With the Large Hadron Collider (LHC) at CERN now taking data at unprecedentedly high energies, the effort to control backgrounds in searches for the Higgs boson and other putative particles is taking on paramount urgency. Recently the dependence of the Higgs boson cross section for the dominant gluon–gluon fusion channel on PDFs has been the cause of some debate [1–3], highlighting the need for a careful determination of strong interaction inputs such as gluon distributions, the strong coupling constant α_s , and higher-order radiative corrections.

At lower energies, the importance of PDF uncertainties has also been discussed recently in fixed-target experiments, particularly for the d quark distribution in the region of large parton momentum fractions x ($x \gtrsim 0.5$) [4, 5]. Because both proton and deuterium deep-inelastic scattering (DIS) data are required to constrain the d quark PDF, uncertainties in the nuclear corrections in the deuteron at large x translate into significant and growing uncertainties on the d/u ratio as $x \rightarrow 1$. Through Q^2 evolution, this can impact cross section calculations at smaller x and larger Q^2 [6], especially in regions where the rapidity is large.

In addition to Higgs boson cross sections, other processes studied at the LHC or the Tevatron at Fermilab that may be sensitive to PDF uncertainties include the production of heavy W' and Z' bosons associated with additional $SU(2) \times U(1)$ gauge groups. These are predicted in various extensions of the Standard Model, such as the $SO(10)$ and E_6 grand unified theories, or supersymmetric models, some with W' and Z' boson masses at the TeV scale (for reviews see, *e.g.*, Refs. [7–10]). Their production cross sections at large rapidities will involve products of PDFs evaluated with one value of x small and the other large, thereby exposing them to uncertainties in PDFs at large x , particularly near the kinematic limits.

In this paper we explore the sensitivity of the weak boson production cross sections to uncertainties in PDFs at large x . For our numerical estimates we use the PDFs from the recent CTEQ-Jefferson Lab (CJ) next-to-leading order (NLO) global analysis [5] of proton and deuteron data, which quantified the model dependence of the nuclear corrections in the deuteron and the resulting effects on the PDFs. In Sec. II we briefly review the CJ analysis

and the origin of the PDF uncertainties, before examining their impact in Sec. III on the physical W^\pm and Z boson cross sections, and W and lepton charge asymmetries. The effects of large- x PDF uncertainties on production rates of heavy W' and Z' bosons in pp and $p\bar{p}$ collisions at the LHC and Tevatron, respectively, are studied in Sec. IV as a function of the boson mass, and limits placed on the accuracy with which cross sections for bosons of a given mass can currently be determined. (Even though data taking has now been completed at the Tevatron, considerable quantities of data remain to be analyzed.) Finally, some concluding remarks are made in Sec. V.

II. PDF UNCERTAINTIES AT LARGE x

The CJ analysis [5] was a dedicated global NLO fit of proton and deuteron DIS and other high-energy scattering data, which critically examined the effects on PDFs of nuclear corrections in the deuteron F_2 structure function. Nuclear corrections were estimated using a smearing function computed within the weak binding approximation [11, 12], taking into account nuclear binding and Fermi motion, as well as a range of models describing the possible modification of the nucleon structure function off-shell [11, 13, 14]. Several deuteron wave functions were considered, based on high-precision nucleon–nucleon potentials, including the nonrelativistic CD-Bonn [15] and AV18 [16] wave functions, and the relativistic WJC-1 and WJC-2 wave functions [17], as well as the older Paris [18] wave function for reference. The off-shell corrections were estimated from a relativistic quark spectator model [14], and from a phenomenological model proposed by Kulagin & Petti [11] but modified for the specific case of the deuteron (see Ref. [5] for details).

Combinations of deuteron wave functions and off-shell models giving the smallest and largest nuclear effects were identified, and used to define the range of the nuclear corrections from the minimum (WJC-1 wave function and no off-shell corrections) to the maximum (CD-Bonn wave function and largest off-shell corrections) nuclear corrections. The central values, which are used as a reference, were obtained using the AV18 wave function and an intermediate off-shell correction. The resulting fitted d/u quark distribution ratio is shown in Fig. 1 for the full range of nuclear uncertainties determined in Ref. [5] (see also Refs. [19, 20]). While the u quark distribution is relatively well constrained by proton structure function data for all values of x , the d quark PDF has large uncertainties beyond $x \approx 0.5$. Significant

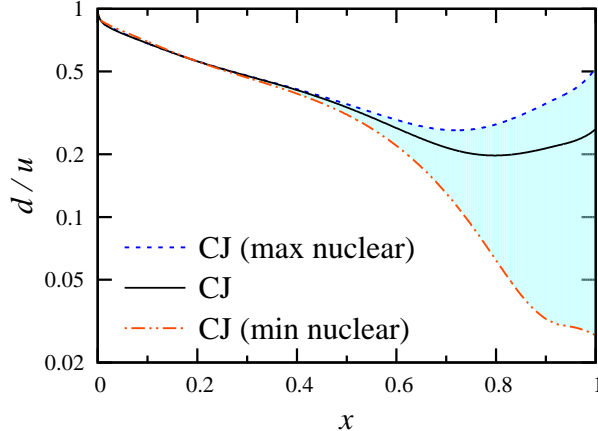


FIG. 1: Ratio of d to u quark distributions for the CJ PDFs [5] at $Q^2 = 10 \text{ GeV}^2$. The shaded band illustrates the uncertainty range between maximum (blue dashed) and minimum (red dot-dashed) nuclear corrections in the deuteron.

uncertainties appear also in the gluon PDF in the region of x not directly constrained by data, as well as in the \bar{u} and \bar{d} distributions due to correlations with the d quark, induced in the global fits by moderate- x jet and dilepton production data, respectively.

Several experiments to directly measure d/u up to $x \approx 0.8$ are planned at the 12 GeV energy upgraded Jefferson Lab in the near future [21–23], which it is hoped will reduce the uncertainties significantly. These include the “MARATHON” [22] experiment, which aims to extract F_2^n/F_2^p from a measurement of the F_2 structure functions of tritium and ^3He with cancellation of nuclear effects to the $\approx 1\%$ level [24], as well as the “BoNuS” experiment [21], which minimizes nuclear corrections in semi-inclusive DIS from deuterium by tagging slow, backward protons that effectively guarantee scattering from a nearly-free neutron. In addition, parity-violating DIS on a hydrogen target [23] will yield a new combination of u and d PDFs at large x , free of any nuclear corrections (see Ref. [5] for further details). In the meantime, however, it is important to establish the limitations that the current uncertainties on the d quark PDF at large x place on the calculation of observables which may be sensitive to these. In the following we shall illustrate the impact of PDF uncertainties at large x arising specifically from the dependence on the model of nuclear corrections in the deuteron. The choice of CJ PDFs for this purpose is merely for convenience, as these are the only PDFs available that explicitly quantify the nuclear model dependence.

III. W AND Z BOSON PRODUCTION

In this section we discuss the effects of PDF uncertainties at large x on the W and Z boson cross sections, and possible constraints on these obtained from measurements at large rapidities. Earlier studies probing the sensitivity of weak boson production to PDF uncertainties were explored in Refs. [25–33]. The discussion here is not meant to provide an exhaustive account of detailed aspects of W boson production, but simply highlight the fact that nuclear corrections in deuterium are an important source of PDF uncertainty at large x that has not been addressed in earlier analyses. To begin with we shall review the general formulas for the inclusive weak boson production cross sections in hadronic collisions relevant to current collider experiments.

A. Cross sections

Hadron–hadron collisions involve at least two interacting partons, one from the hadron “beam” and one from the “target”, with momentum fractions x_1 and x_2 , respectively. At fixed center of mass energy \sqrt{s} and boson rapidity

$$y = \frac{1}{2} \ln \left(\frac{E + p_z}{E - p_z} \right), \quad (1)$$

where E and p_z are the boson energy and longitudinal momentum in the hadron center of mass frame, the parton momentum fractions are given (at leading order in the strong coupling constant) by

$$x_{1,2} = \frac{M}{\sqrt{s}} e^{\pm y}, \quad (2)$$

where M is the mass of the produced boson. The absolute value of the rapidity thus ranges from 0 up to $|y|_{\max} = \log(\sqrt{s}/M)$. For inclusive W^+ production in pp or $p\bar{p}$ collisions, for example, the cross sections (to leading order and neglecting heavy quarks) are given by [34]

$$\begin{aligned} \frac{d\sigma}{dy} (pp \rightarrow W^+ X) = & \frac{2\pi G_F}{3\sqrt{2}} x_1 x_2 \left(\cos^2 \theta_C [u(x_1)\bar{d}(x_2) + \bar{d}(x_1)u(x_2)] \right. \\ & \left. + \sin^2 \theta_C [u(x_1)\bar{s}(x_2) + \bar{s}(x_1)u(x_2)] \right), \end{aligned} \quad (3a)$$

$$\begin{aligned} \frac{d\sigma}{dy} (p\bar{p} \rightarrow W^+ X) = & \frac{2\pi G_F}{3\sqrt{2}} x_1 x_2 \left(\cos^2 \theta_C [u(x_1)d(x_2) + \bar{d}(x_1)\bar{u}(x_2)] \right. \\ & \left. + \sin^2 \theta_C [u(x_1)s(x_2) + \bar{s}(x_1)\bar{u}(x_2)] \right), \end{aligned} \quad (3b)$$

where G_F is the Fermi constant, and θ_C is the Cabibbo mixing angle. The W^- differential cross sections are similar to those in Eqs. (3), but with quark PDFs replaced by the corresponding antiquark PDFs. Consequently the W^\pm cross sections in $p\bar{p}$ collisions are related by $(d\sigma_{W^+}/dy)(y) = (d\sigma_{W^-}/dy)(-y)$, and hence are equivalent when integrated over rapidity. For pp collisions the individual W^+ and W^- cross sections are symmetric with respect to $y \rightarrow -y$, but otherwise unrelated.

Similarly, the leading order, light quark cross sections for Z boson production in pp or $p\bar{p}$ collisions are given by [34]

$$\frac{d\sigma}{dy}(pp \rightarrow ZX) = \frac{2\pi G_F}{3\sqrt{2}} \sum_q \left[(g_V^q)^2 + (g_A^q)^2 \right] x_1 x_2 (q(x_1)\bar{q}(x_2) + \bar{q}(x_1)q(x_2)), \quad (4a)$$

$$\frac{d\sigma}{dy}(p\bar{p} \rightarrow ZX) = \frac{2\pi G_F}{3\sqrt{2}} \sum_q \left[(g_V^q)^2 + (g_A^q)^2 \right] x_1 x_2 (q(x_1)q(x_2) + \bar{q}(x_1)\bar{q}(x_2)), \quad (4b)$$

where $g_V^q = t_3^q - 2e_q \sin^2 \theta_W$ and $g_A^q = t_3^q$ are the vector and axial-vector couplings of the Z boson to quark q [35], with e_q and t_3^q the electromagnetic charge and weak isospin of the quark, respectively, and θ_W the weak mixing angle. The symmetry properties of the differential Z cross sections are such that $(d\sigma_Z/dy)(y) = (d\sigma_Z/dy)(-y)$ for both pp and $p\bar{p}$ collisions. Note that in the conventions of Ref. [34] the couplings $g_{V,A}^q$ are two times smaller than the standard ones in Ref. [35]. In the convention used here the couplings $(g_V^q)^2 + (g_A^q)^2$ in Eqs. (4) are equal to $5/18 + \Delta(1 + \Delta)/9$ and $13/36 + \Delta(1 + \Delta/4)/9$ for u and d quarks, respectively, where $\Delta = 1 - 4\sin^2 \theta_W$. Since $\Delta \approx 0$, the effective strengths of the Z boson couplings to u and d quarks are therefore similar.

While the expressions in Eqs. (3) and (4) are given at leading order, in practice we compute all cross sections at NLO, including heavy quarks. The leading order expressions give the dominant contributions, however, and are instructive in clearly illustrating that in pp collisions, for instance, the W^+ cross section at large rapidity is mostly dependent on the u quark, while the W^- cross section depends mostly on the d . Since the nuclear corrections discussed in Sec. II induce the greatest uncertainty into the large- x d quark PDF, one can immediately deduce that W^- production in pp scattering will be most affected by these uncertainties, while W^+ production will be relatively inert. For $p\bar{p}$ collisions, the large- x PDF uncertainties will affect W^- cross sections at large positive rapidities, or equivalently W^+ cross sections at negative rapidities.

In the following sections we will compute the W and Z boson cross sections numerically

to study their sensitivity to PDF uncertainties at large x . All calculations will be for pp collisions at the LHC with $\sqrt{s} = 7$ TeV, and for $p\bar{p}$ collisions at the Tevatron with $\sqrt{s} = 1.96$ TeV.

B. Z bosons

The sensitivity of the differential Z boson cross section to the different PDF behaviors at large x is illustrated in Fig. 2 as a function of the Z boson rapidity y_Z , for LHC and Tevatron kinematics. The cross sections are computed from the CJ PDFs [5] with minimal and maximal nuclear corrections, relative to a reference cross section computed from the central PDFs as described in Sec. II.

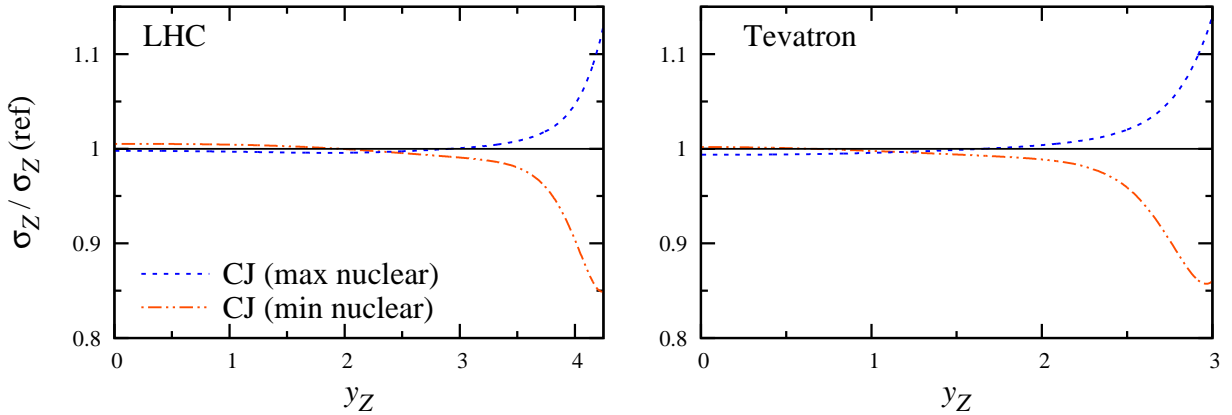


FIG. 2: Differential Z boson cross section as a function of the Z rapidity y_Z , computed from CJ PDFs with maximum (blue dashed) and minimum (red dot-dashed) nuclear corrections, relative to the reference cross section $\sigma_Z(\text{ref})$ calculated using the central CJ PDF set [5]. The cross sections are computed for pp collisions at the LHC with $\sqrt{s} = 7$ TeV (**left**) and for $p\bar{p}$ collisions at the Tevatron with $\sqrt{s} = 1.96$ TeV (**right**).

The behavior of the cross section ratios is qualitatively similar at both the LHC and the Tevatron, with the main difference being the range of rapidities accessible from the respective available energies \sqrt{s} . At low rapidities the cross sections are relatively insensitive to uncertainties in the large- x PDFs, with differences of $\lesssim 1\%$ for $y_Z \lesssim 3$ at the LHC and $y_Z \lesssim 2$ at the Tevatron. At larger rapidities, however, there is far greater sensitivity to the large- x behavior, particularly of the d quark, leading to $\approx 15\%$ uncertainty in the differential cross section for $y_Z = 4$ at the LHC, and for $y_Z = 2.8$ at the Tevatron, which correspond to

parton fractions of $x \approx 0.7$. As one approaches the kinematical thresholds of $y_{Z,\text{max}} \approx 4.3$ at the LHC and $y_{Z,\text{max}} \approx 3.1$ at the Tevatron, these uncertainties increase dramatically, as would be expected from the $x \rightarrow 1$ behavior of the d/u ratio in Fig. 1.

C. W cross sections and asymmetries

The behavior of the W boson differential cross sections as a function of the W rapidity y_W is qualitatively similar to those for the Z , but with some important differences, as Fig. 3 illustrates for W^+ and W^- production at LHC and Tevatron kinematics. Again, there is very little dependence on the large- x PDF uncertainties at low rapidity, but increasing sensitivity as the rapidity approaches its kinematic upper limit of $y_{W,\text{max}} \approx 4.5$ at the LHC and $y_{Z,\text{max}} \approx 3.2$ at the Tevatron.

For W^+ bosons, the cross section maintains relatively little dependence on the large- x nuclear corrections over the entire rapidity range, barely reaching 4% difference at $y_W \approx 4$ at the LHC, or $y_W \approx 3$ at the Tevatron. In contrast, the W^- cross section shows an even stronger dependence on nuclear corrections than the Z cross section in Fig. 2, deviating significantly from unity for $y_W \gtrsim 3$ for the LHC and $y_W \gtrsim 2$ for the Tevatron, and reaching upwards of 40% deviation at $y_W \approx 4$ and 3 for LHC and Tevatron kinematics, respectively. The greater sensitivity of the W^- production cross section compared with the W^+ can be understood from the dominance of the latter by the u quark PDF at large x , which is relatively insensitive to the nuclear correction uncertainties. The enhancement of the W^- cross section at large y_W for the CJ PDFs with maximum nuclear corrections, and corresponding suppression of the CJ PDFs with minimum nuclear corrections, relative to the central CJ fits essentially follows the trend of the d quark PDF in Fig. 1. The slight enhancement of the W^+ cross section at large y_W for the CJ PDFs with minimum nuclear corrections reflects the anticorrelation of the u quark PDF with respect to the d observed in Ref. [5].

Taking differences and sums of the W^+ and W^- cross sections, one can construct the W boson asymmetry,

$$A_W = \frac{\sigma_{W^+}(y) - \sigma_{W^-}(y)}{\sigma_{W^+}(y) + \sigma_{W^-}(y)}, \quad (5)$$

where $\sigma_{W^\pm}(y) \equiv d\sigma_{W^\pm}/dy$. The asymmetry is shown in Fig. 4 versus the W rapidity at the LHC and Tevatron for the CJ PDFs with maximum and minimum nuclear corrections.

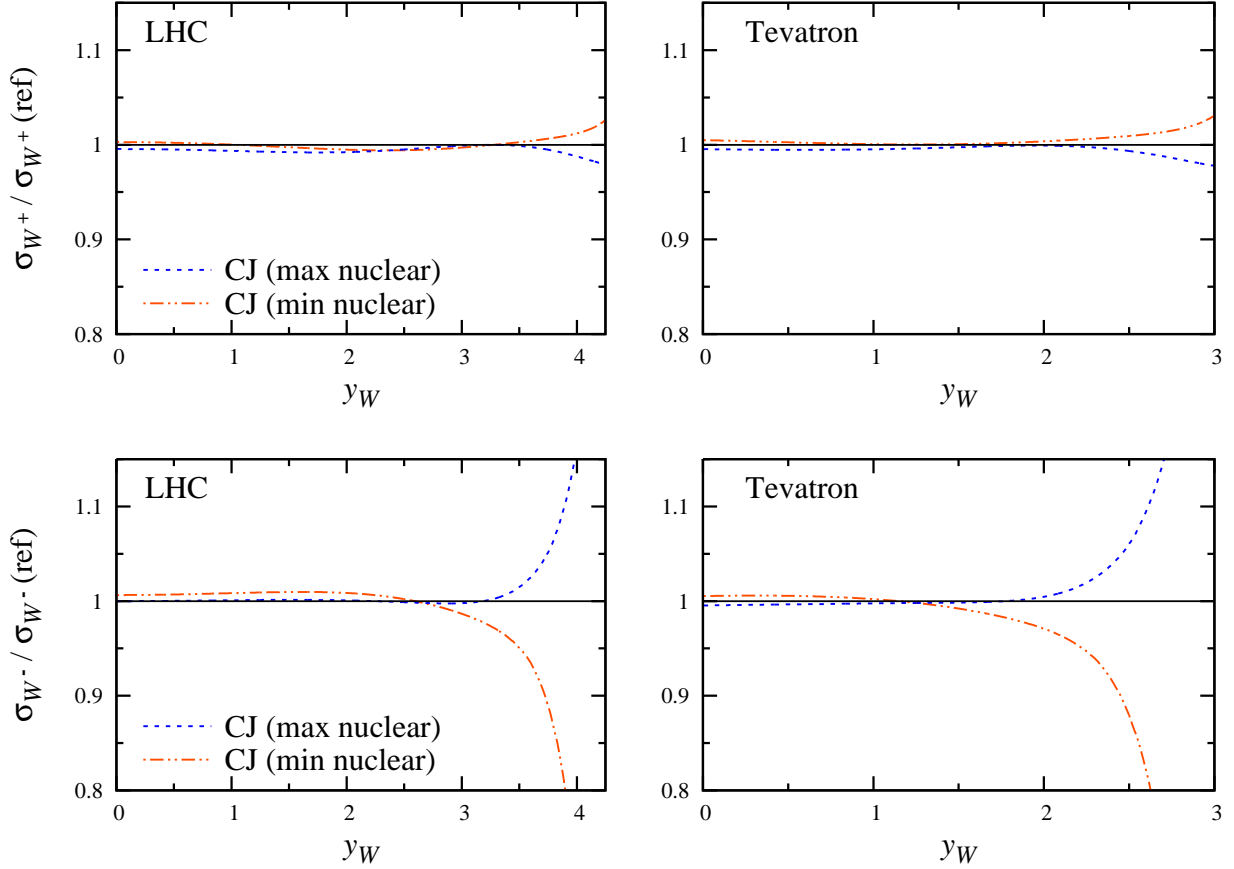


FIG. 3: Differential W^+ (**top**) and W^- (**bottom**) boson cross sections as a function of the W rapidity y_W , computed from CJ PDFs with maximum (blue dashed) and minimum (red dot-dashed) nuclear corrections, relative to the reference cross sections $\sigma_{W^\pm}(\text{ref})$ calculated using the central CJ PDF set [5]. The cross sections are computed for pp collisions at the LHC with $\sqrt{s} = 7$ TeV (**left**) and for $p\bar{p}$ collisions at the Tevatron with $\sqrt{s} = 1.96$ TeV (**right**).

A clear deviation between the two PDF fits becomes visible at $y_W \gtrsim 3.5$ for the LHC and $y_W \gtrsim 2$ for the Tevatron, corresponding to one of the partons carrying momentum fractions $x \approx 0.4$ and $x \approx 0.35$, respectively. Data on W boson asymmetries may therefore provide constraints on the d/u quark distribution ratio already at these moderate values of x . In particular, comparison with the CDF data [36] in Fig. 4 illustrates a preference for larger A_W values at $y_W \gtrsim 2$, which corresponds to $x_1 \gg x_2$. As observed in Ref. [5], since the asymmetry at large y_W can be approximated by

$$A_W \approx \frac{d(x_2)/u(x_2) - d(x_1)/u(x_1)}{d(x_2)/u(x_2) + d(x_1)/u(x_1)}, \quad [x_1 \gg x_2], \quad (6)$$

this would suggest a smaller d/u ratio at large x_1 , as would arise for the CJ PDFs with

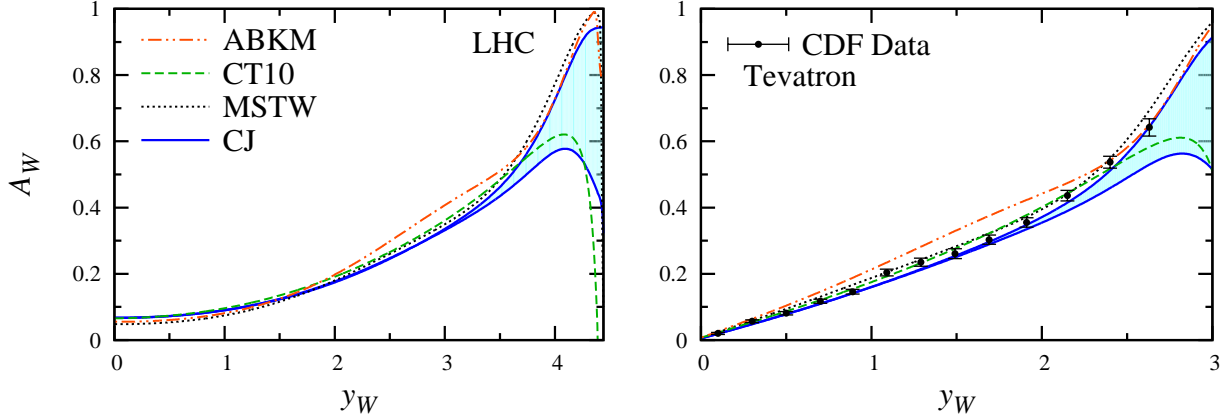


FIG. 4: W boson asymmetry A_W as a function of the W rapidity y_W at LHC (**left**) and Tevatron (**right**) kinematics, computed from CJ PDFs [5] with minimum (upper blue solid) and maximum (lower blue solid) nuclear corrections. For comparison, the asymmetries using the ABKM [29] (red dot-dashed), CT10 [30] (green dashed) and MSTW [31] (black dotted) PDF sets are also shown.

minimum nuclear corrections.

For comparison, the asymmetries calculated from the ABKM [29], CT10 [30] and MSTW [31] PDF sets are also shown in Fig. 4. Each parametrization shows good agreement with the Tevatron CDF data, with the exception of the ABKM fit, which overestimates the asymmetries at intermediate rapidities, $y_W \approx 1 - 2$. This may be due to the W asymmetry data not being fitted directly in the ABKM analysis. At large rapidity the spread in the various PDF sets is comparable to the difference between the CJ PDFs with minimal and maximal nuclear corrections. However, we stress that the origin of the differences between the PDF sets is unrelated to the difference between the two CJ PDF sets. Had the various non-CJ PDFs sets included nuclear uncertainties in their analysis, each one would have a corresponding nuclear uncertainty band similar to the one in Fig. 4, and the combined spread between them would subsequently be significantly larger.

D. Lepton Asymmetries

Experimentally, measurement of W bosons asymmetries requires reconstruction of the W boson distributions from their leptonic decays, $W^+ \rightarrow l^+ \nu_l$ and $W^- \rightarrow l^- \bar{\nu}_l$, with $l = e$ or μ . On the other hand, lepton charge asymmetries can be constructed directly from the W^\pm

decay products and studied as a function of the lepton pseudorapidity η , defined as

$$\eta = \frac{1}{2} \ln \left(\frac{|\mathbf{k}| + k_z}{|\mathbf{k}| - k_z} \right) = -\ln \tan \frac{\theta}{2}, \quad (7)$$

where \mathbf{k} is the charged lepton momentum, and θ is the angle between the lepton momentum and the beam axis in the center of mass frame. The lepton asymmetry is then given by

$$A_\eta = \frac{\sigma_{l^+}(\eta) - \sigma_{l^-}(\eta)}{\sigma_{l^+}(\eta) + \sigma_{l^-}(\eta)}, \quad (8)$$

where $\sigma_{l^\pm}(\eta) \equiv d\sigma_{l^\pm}/d\eta$ is the differential cross section for the production and leptonic decay of the W^\pm .

Lepton asymmetry data from the D0 Collaboration [37] at Fermilab are shown in Fig. 5 as a function of the pseudorapidity up to $\eta \approx 2.5$. The data are integrated over lepton transverse momenta $p_T > 25$ GeV, and compared with asymmetries computed from the CJ PDFs with maximum and minimum nuclear corrections using the MCFM (Monte Carlo for FeMtobarn processes) program [38]. Good agreement is obtained between the calculated asymmetry and data, although little sensitivity is evident to the large- x nuclear uncertainty in the PDFs observed in Fig. 4 until $\eta \approx 3$.

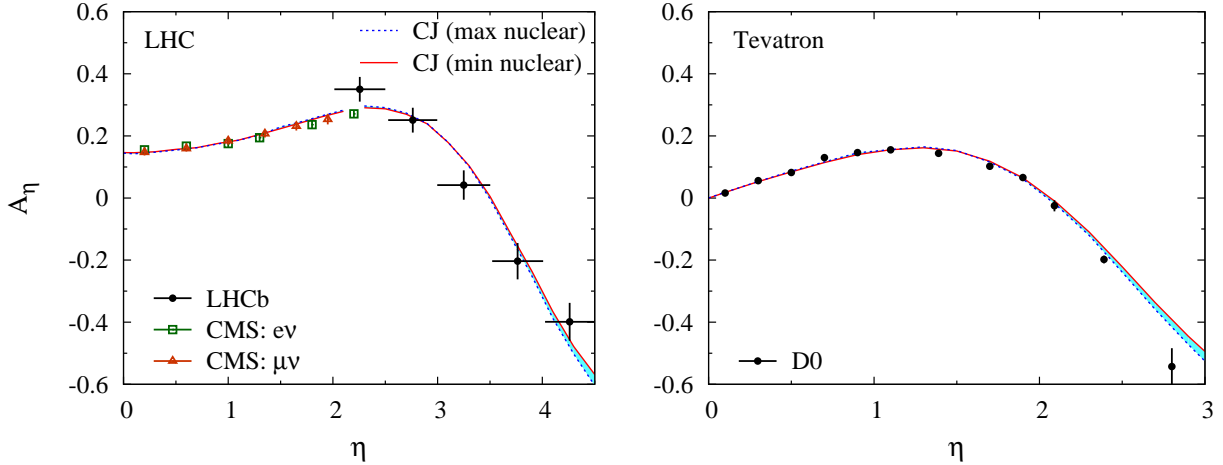


FIG. 5: Lepton charge asymmetry A_η as a function of lepton pseudorapidity η at the LHC (**left**) and Tevatron (**right**), computed from CJ PDFs [5] with maximum (blue dotted) and minimum (red solid) nuclear corrections. The calculations are compared with CMS $W \rightarrow e\nu_e$ (red squares) and $W \rightarrow \mu\nu_\mu$ (blue triangles) data for a lepton transverse momentum cut $p_T > 25$ GeV [40], and preliminary LHCb data (black circles) for $p_T > 20$ GeV [41], as well as with D0 data from the Tevatron $p_T > 25$ GeV [37].

Similar behavior is found for the new lepton charge asymmetry data from the LHC. Here lepton asymmetries have been measured by the ATLAS [39] and CMS [40] Collaborations for pseudorapidities $|\eta| \lesssim 2$, and preliminary results from the LHCb Collaboration [41] extend the coverage to $2 \lesssim \eta \lesssim 4.5$ [42]. The agreement of the CJ PDFs with the LHC data is good over the entire range of η , as Fig. 5 illustrates for CMS $W \rightarrow e\nu$ and $W \rightarrow \mu\nu$ data integrated over lepton transverse momenta $p_T > 25$ GeV, and LHCb data with $p_T > 20$ GeV. The dependence on the large- x behavior of PDFs, however, becomes visible only for $\eta \gtrsim 4$.

The limited sensitivity of the lepton asymmetries to large- x PDFs is not surprising, given that the lepton asymmetry is computed by convoluting the W boson cross sections with the W boson decay distributions, which dilutes the sensitivity to regions where the PDFs are small. Although the lepton asymmetry data are clearly valuable for constraining global PDF fits in general, greater sensitivity to the large- x behavior of the d/u ratio may be possible through the reconstruction of the W boson asymmetries themselves. Note, however, that the reconstruction of W boson asymmetries is limited by theoretical uncertainties such as the modeling of the p_T distributions and higher-order resummation corrections (which also affect the lepton asymmetries), as well as the choice of PDFs used to compute the event reweighting coefficients in the reconstruction.

IV. HEAVY W' AND Z' BOSONS

The production rate of any new heavy boson beyond the Standard Model will naturally depend on its internal properties such as the spin. Many possibilities have been canvassed for how such heavy bosons can arise [9], including as scalar excitations in R -parity violating supersymmetry [43], spin-1 Kaluza-Klein excitations of Standard Model gauge bosons in the presence of extra dimensions [44], or as spin-2 excitations of the graviton [45]. On the other hand, if the new bosons are associated with extensions of the Standard Model gauge group, their interactions with fermions will resemble those of the W and Z bosons of the electroweak theory, with different masses and couplings.

In this section we explore this latter possibility, and in particular the sensitivity of the production cross sections to uncertainties in PDFs at large x . From Eq. (2) one can see that increasing the mass will directly increase the relevant x values, so that higher mass bosons will more readily sample the high- x region where the nuclear uncertainties are more

prominent. In the calculations discussed here we shall assume that the putative W' and Z' bosons have the same properties as the Standard Model W and Z bosons, except for their larger masses. The cross sections will of course decrease rapidly with increasing boson mass, so that the effects of the large- x PDF uncertainties will become more significant as the mass increases. Of course the details of the predictions will change in more sophisticated models in which the W' and Z' couplings are different from those in the Standard Model; however, the simplified scenario considered here is sufficient to illustrate the possible impact of large- x PDF uncertainties on new physics searches.

Currently the exclusion limit on the W' mass from the Tevatron, for couplings similar to Standard Model couplings, is $M_{W'} > 1.12$ TeV at the 95% confidence level with an integrated luminosity of 5.3 fb^{-1} [46]. For the neutral Z' boson the limits vary between $M_{Z'} \gtrsim 800$ GeV and $M_{Z'} \gtrsim 1$ TeV [47], depending on the Standard Model extension considered [35]. The latest results from the LHC place the limits for the W' mass at $M_{W'} > 2.15$ TeV [48] and for the Z' mass at $M_{Z'} > 1.83$ TeV [49] in the Sequential Standard Model, with the same couplings to fermions as for the W and Z . A similar constraint on the Z' mass in grand unified theories is also obtained from measurements of atomic parity violation in ^{133}Cs [50].

A. Rapidity distributions

The differential cross sections for heavy W' and Z' bosons will generally have similar behavior as a function of rapidity to those of the physical boson cross sections in Figs. 2 and 3, except for a smaller rapidity range, with the large- x region emphasized more strongly for increasing boson mass. According to the study by Erler *et al.* [51], pp collisions at the LHC with $\sqrt{s} = 7$ TeV will be sensitive to Z' masses up to $M_{Z'} \approx 2.1 - 2.7$ TeV for luminosities between 30 fb^{-1} and 300 fb^{-1} , corresponding to the so-called “low-luminosity” and “high-luminosity” LHC scenarios, respectively. (With $\sqrt{s} = 14$ TeV the mass limits would vary between $M_{Z'} \approx 3.6$ and 4.6 TeV.) For $p\bar{p}$ collisions at the Tevatron, an energy of $\sqrt{s} = 2$ TeV with a luminosity of 10 fb^{-1} would be expected to allow sensitivity to Z' masses up to ≈ 1 TeV [51]. In this section we therefore consider Z' (and W') masses up to 1 TeV and 3 TeV for Tevatron and LHC kinematics, respectively.

From Eq. (2), larger boson masses naturally restrict the kinematically accessible range of rapidities, so that at the LHC, for example, a 1 TeV (3 TeV) Z' boson can be produced at

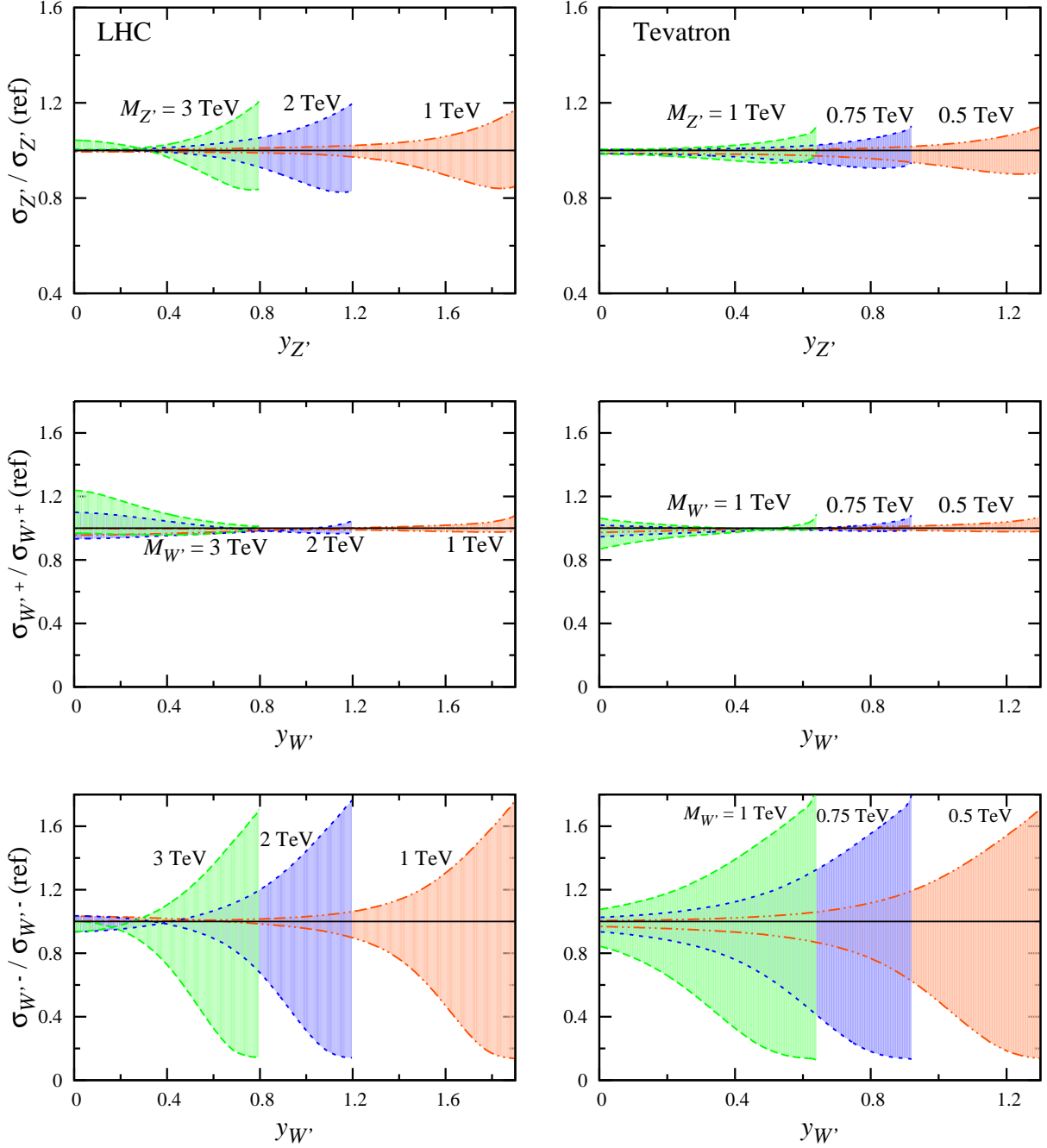


FIG. 6: Differential Z' (**top**), W'^+ (**center**) and W'^- (**bottom**) cross sections as a function of the rapidity, computed from CJ PDFs with maximum and minimum nuclear corrections, relative to the reference cross sections $\sigma_{Z',W'}(\text{ref})$ calculated using the central CJ PDF set [5]. The LHC cross sections (**left**) are computed for boson masses $M_{Z',W'} = 1$ TeV (red dot-dashed), 2 TeV (short-dashed) and 3 TeV (long-dashed) with $\sqrt{s} = 7$ TeV, while the Tevatron ratios (**right**) are shown for $M_{Z',W'} = 0.5$ TeV (red dot-dashed), 0.75 TeV (short-dashed) and 1 TeV (long-dashed) with $\sqrt{s} = 1.96$ TeV.

a maximum rapidity of $|y_{Z'}|_{\max} = 2.0$ (0.9), compared with $|y_Z|_{\max} = 4.3$ for the Standard Model Z boson. The kinematic reach and sensitivity to large- x PDFs is illustrated in Fig. 6 (top) for the differential Z' cross section ratio as a function of $y_{Z'}$, for masses $M_{Z'} = 1, 2$ and 3 TeV at the LHC, and $M_{Z'} = 0.5, 0.75$ and 1 TeV at the Tevatron. As the rapidities approach their kinematical thresholds for a given $M_{Z'}$, the uncertainty in the differential cross sections increases significantly, reaching about 30 – 40% of the central CJ value for pp collisions at the LHC, and 15 – 20% for $p\bar{p}$ collisions at the Tevatron.

Because the couplings of the Z' to u and d quarks are assumed to be similar (see Sec. III A), the Z' cross section at the LHC depends on both the combinations $u(x_1)\bar{u}(x_2) + \bar{u}(x_1)u(x_2)$ and $d(x_1)\bar{d}(x_2) + \bar{d}(x_1)d(x_2)$. However, since the d/u and \bar{u}/u ratios are $\ll 1$ at large x values, which are preferentially sampled for large $M_{Z'}$, the contributions of d quarks are suppressed relative to u quarks. Consequently the Z' ratios in Fig. 6 are only mildly affected by uncertainties in quark PDFs at large x . The Z' production cross section in $p\bar{p}$ collisions at the Tevatron, on the other hand, is determined predominantly by the product $u(x_1)u(x_2)$, which is well constrained and independent of the nuclear model for all $x_{1,2}$, and therefore has an even smaller uncertainty.

For the W' differential cross sections, the behavior as a function of $y_{W'}$ is qualitatively different for W'^+ and W'^- production, shown in Fig. 6 (center) and (bottom), respectively, with the latter displaying dramatically greater sensitivity to large- x PDF uncertainties. This is clear from Eqs. (3), where for pp collisions the dominant contribution to the W'^+ cross section depends on the products $u(x_1)\bar{d}(x_2)$ and $\bar{d}(x_1)u(x_2)$. While the u quark PDF is insensitive to the nuclear corrections, the \bar{d} distribution varies considerably with the nuclear model, especially at larger values of x . At high rapidity the \bar{d}/u ratio is small, and the cross section is determined by the u PDF with x_1 large and the \bar{d} PDF with x_2 small, both of which are well constrained. For $y_{W'} \rightarrow 0$, on the other hand, one has $x_1 = x_2 \approx 0.14$ for $M_{W'} = 1$ TeV and $x_1 = x_2 \approx 0.42$ for $M_{W'} = 3$ TeV, at which the \bar{d} PDF has significantly greater uncertainty than the u , yielding up to $\approx 25\%$ uncertainties in the cross section. Similarly for $p\bar{p}$ collisions at the Tevatron, the W'^+ cross section is dominated by the combination $u(x_1)d(x_2)$, which for $x_1 \gg x_2$ at high rapidity is relatively well constrained. At central rapidity, with $x_1 = x_2 \approx 0.25$ (0.5) for $M_{W'} = 0.5$ (1) TeV, the uncertainties in the cross section remain within the $\approx 10\%$ level.

In contrast, the W'^- cross section at high rapidity is determined by the products

$d(x_1)\bar{u}(x_2)$ and $\bar{u}(x_1)d(x_2)$ in pp collisions, and $d(x_1)u(x_2)$ and $u(x_1)d(x_2)$ in $p\bar{p}$ collisions. Consequently, uncertainties in the cross sections at large rapidity, both at the LHC and the Tevatron, arise mainly from the d quark at large x , and exceed 100% as the kinematic limit in y_W is approached. Qualitatively, the growing uncertainty of the W'^- cross section with increasing rapidity resembles the W^- cross section ratio at large y_W in Fig. 3. At central rapidity, the uncertainty in the pp cross section at the LHC is of the order 10%, arising mainly from the uncertainty in the \bar{u} distribution. At the Tevatron, the $p\bar{p}$ cross section is well constrained for small boson mass, but for $M_{W'} > 0.75$ TeV, with $x_1 = x_2 \gtrsim 0.3$, becomes increasingly sensitive to uncertainties in the d quark PDF, reaching about 20% for $M_{W'} = 1$ TeV.

B. Integrated cross sections

Integrating over all rapidities, the resulting total Z' cross section computed from CJ PDFs with minimum and maximum nuclear corrections is shown in Fig. 7 as a function of the Z' mass. Relatively little dependence on the PDFs is observed, with effects of $\lesssim 3\%$ observed for $M_{Z'} < 3$ TeV at the LHC and $M_{Z'} < 1$ TeV at the Tevatron. This is not surprising given that total cross sections are dominated by contributions from low values of $y_{Z'}$, where the PDF uncertainties are generally smaller than at high values of $y_{Z'}$, at which the contributions are suppressed by the steeply falling PDFs as $x \rightarrow 1$. At larger $M_{Z'}$ values the uncertainties generally increase, but are subject to greater fluctuations in the antiquark distributions at high x , and hence are less reliable.

The integrated cross sections for W' bosons in Fig. 8 show somewhat greater sensitivity to large- x PDFs as a function of $M_{W'}$. For W'^+ bosons produced in pp collisions at the LHC the uncertainties increase from $\lesssim 5\%$ for $M_{Z'} = 1$ TeV to $\approx 20\%$ for $M_{Z'} = 3$ TeV. This behavior stems directly from the increasing uncertainty in the \bar{d} antiquark PDF at large x apparent in the W'^+ rapidity distribution at low $y_{W'}$ in Fig. 6. For W'^- boson production in pp scattering, the uncertainties in the total cross section are smaller than for the W'^+ at low $M_{W'}$, remaining $\lesssim 2\%$ for $M_{W'} < 2$ TeV, but increase to $\approx 10\%$ at $M_{W'} = 3$ TeV due to the uncertainty in the \bar{u} quark. The stronger dependence on the behavior of the d quark PDF at large x apparent in the W'^- differential cross section at high rapidity in Fig. 6 is mostly washed out in the integrated cross section.

Because the W' cross sections in $p\bar{p}$ collisions at the Tevatron are determined by the products $u(x_1)d(x_2)$ and $d(x_1)u(x_2)$ for W'^+ and W'^- , respectively, integrating over rapidity samples all accessible values of x_1 and x_2 , so that the total W'^+ and W'^- cross sections are equivalent. The dependence of the integrated W' cross sections on PDFs essentially follows the d quark distribution. For masses $M_{W'} \lesssim 0.5$ TeV there is little sensitivity to the large- x behavior of the PDFs, with $\lesssim 5\%$ uncertainty in the cross section ratio, but increasing dependence at larger $M_{W'}$, with $\approx 30\%$ uncertainty at $M_{W'} = 1$ TeV.

While the sensitivity of the W' and Z' cross sections to the large- x behavior of PDFs increases with increasing W' and Z' masses, the absolute values of the cross sections naturally fall with increasing masses, some 3 orders of magnitude from 100 GeV to 3 TeV. This is illustrated in Fig. 9, where the ratio of the integrated $W'^+ + W'^-$ cross sections computed from CJ PDFs with minimum and maximum nuclear corrections, relative to the cross section with the central CJ PDFs, is plotted versus the integrated Z' cross section. Here the ratio of the W' to Z' masses is kept constant in order to study the effect of the increasing W', Z' mass. For larger boson masses the impact of the large- x PDF uncertainties clearly increases, reflecting the trend observed in Figs. 7 and 8. Note that because the integrated W'^+ cross section is generally larger than the W'^- cross section (because of the larger u distribution compared with the d), the $\sigma_{W'}/\sigma_{W'}(\text{ref})$ ratio in Fig. 9 generally follows the ratio of the W'^+

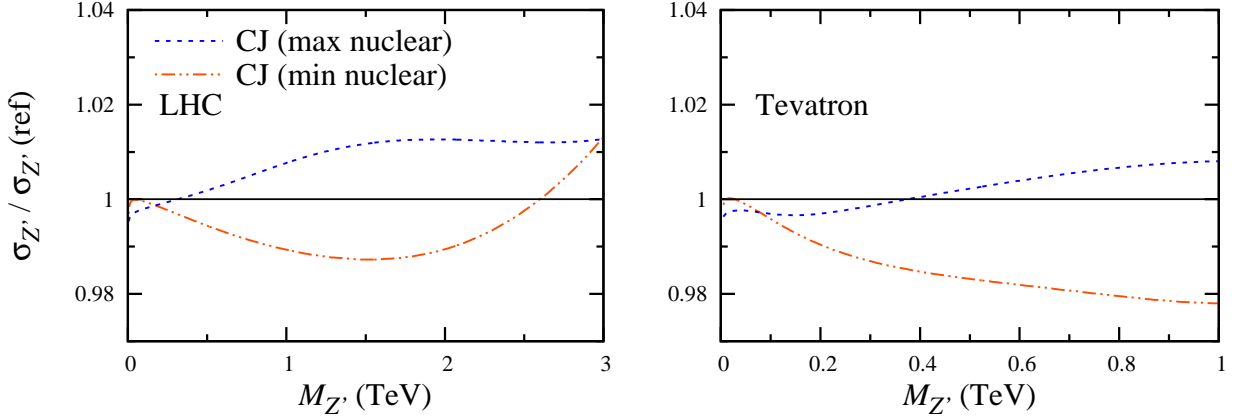


FIG. 7: Integrated Z' boson cross section from Fig. 6 as a function of the Z' mass, computed from CJ PDFs with minimum (red dot-dashed) and maximum (blue dashed) nuclear corrections, relative to the reference cross section $\sigma_{Z'}(\text{ref})$ calculated using the central CJ PDF set [5], for LHC (**left**) and Tevatron (**right**) kinematics.

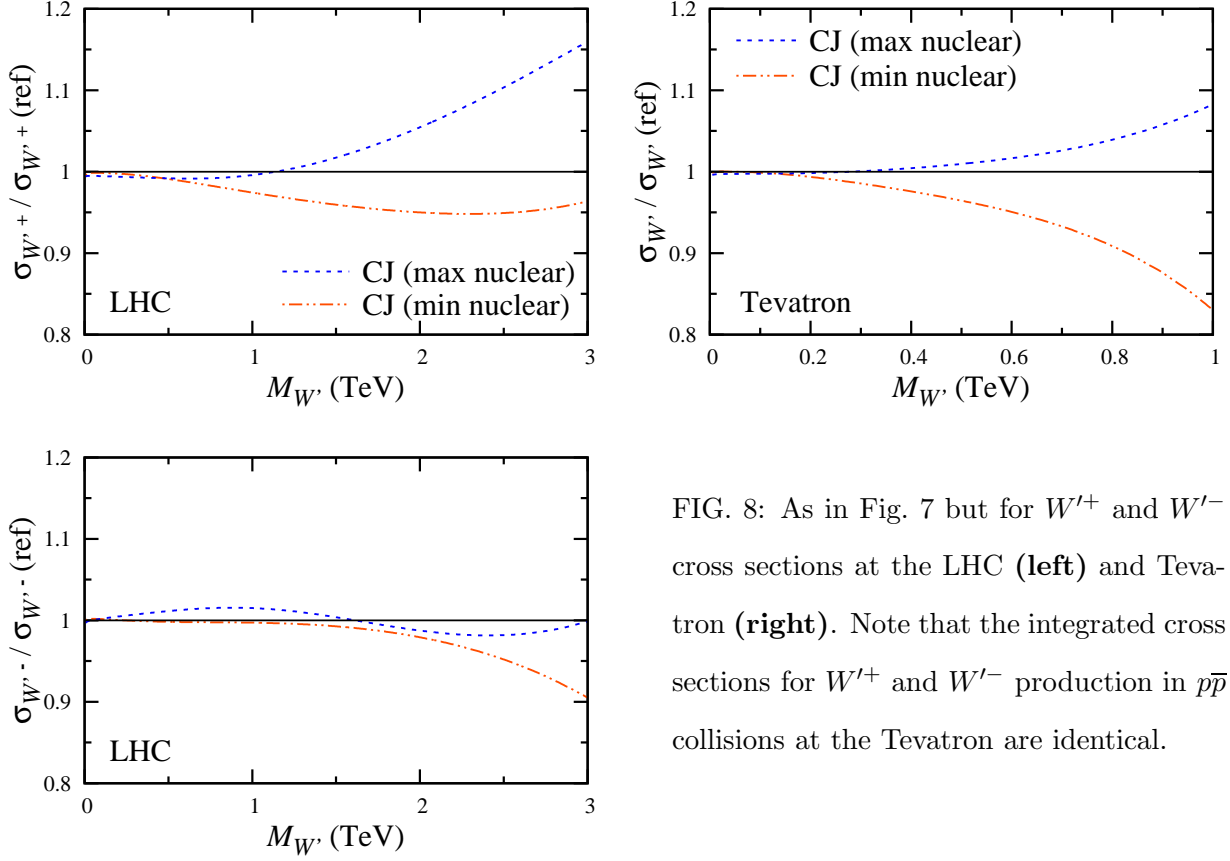


FIG. 8: As in Fig. 7 but for W'^{+} and W'^{-} cross sections at the LHC (**left**) and Tevatron (**right**). Note that the integrated cross sections for W'^{+} and W'^{-} production in $p\bar{p}$ collisions at the Tevatron are identical.

cross sections in Fig. 8 for increasing boson mass.

V. CONCLUSION

In this paper we have explored the sensitivity of weak boson production in hadronic collisions to parton distributions at large values of x . At present there are large uncertainties in the d quark distribution, particularly above $x \approx 0.5$, arising from the model dependence of nuclear corrections used when analyzing deuteron DIS data in global PDF fits, which can impact cross section measurements at large rapidities. The PDF uncertainties can also affect production cross sections of heavy W' and Z' bosons beyond the Standard Model at central rapidities.

Using PDFs extracted from the recent CJ global fit [5], we find increasing sensitivity to the large- x region for Z boson production in $p\bar{p}$ collisions at the Tevatron for Z rapidities

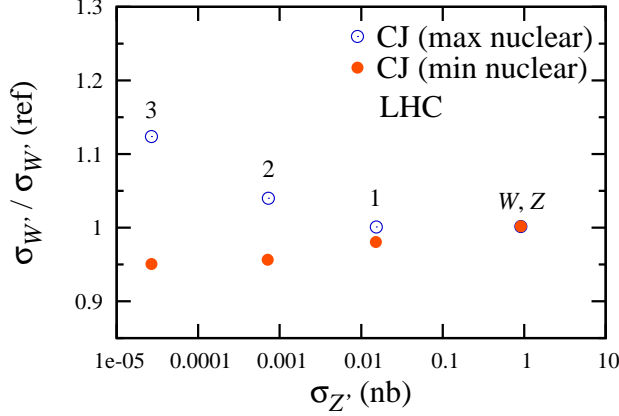


FIG. 9: Ratio of W' boson cross sections $\sigma_{W'}/\sigma_{W'}(\text{ref})$, where $\sigma_{W'} = \sigma_{W'^+} + \sigma_{W'^-}$, versus the Z' boson cross section $\sigma_{Z'}$ for varying Z' boson masses, indicated by the numbers (in TeV) next to the points (the points corresponding to the physical W and Z cross sections are labeled by “ W, Z ”). The cross sections are computed from CJ PDFs with minimum (filled red circle) and maximum (open blue circle) nuclear corrections, relative to the reference cross section calculated from the central CJ PDFs [5].

$y_Z \gtrsim 2$, and in pp collisions at the LHC for $y_Z \gtrsim 3$. Precision measurements of Z boson cross sections at these rapidities, at the Tevatron and particularly at the LHC with the LHCb experiment, will be required to impact global fits of the d quark and constrain nuclear model uncertainties.

For charged weak bosons, the W^+ cross sections are mostly independent of PDF uncertainties due to their preferential coupling to u quarks, whereas the W^- cross sections display strong dependence on the d quark uncertainties for W rapidities $y_W \gtrsim 1.5$ at Tevatron and $y_W \gtrsim 3$ at LHC kinematics. Measurements of W boson charge asymmetries at large rapidities, such as those from the CDF Collaboration at Fermilab [36], thus provide strong constraints on the behavior of the d/u ratio at large x , although such measurements are very challenging given the low rates expected in the relevant regions of kinematics. Direct reconstruction of W boson asymmetries in the LHCb experiment for $\sqrt{s} = 7$ TeV would also be extremely valuable in providing access to PDFs at $x \approx 1$. We have also compared charged lepton asymmetries with data from D0 [37], and from the CMS [40] and LHCb Collaborations [41] at the LHC, finding good overall agreement with the CJ PDFs, but weak sensitivity to large- x PDFs.

The large- x PDF uncertainties also affect the production rates of heavy W' and Z' bosons, and the impact of these was studied as a function of the boson mass for Standard Model couplings. At high rapidity, the W'^+ cross section in pp and $p\bar{p}$ collisions is mostly sensitive to the u quark PDF at large x and therefore well constrained. The Z' cross section displays a mild sensitivity to the d quark PDF at large x , reaching upwards of 40% uncertainty at the kinematic rapidity limit. The effects are even more pronounced for W'^- cross sections, where the uncertainties exceed 100% at large y_W .

At central rapidity the Z' cross section is well constrained, with weak sensitivity to \bar{u} and \bar{d} quarks at the LHC for $M_{Z'} < 3$ TeV. The W' central rapidity cross sections, on the other hand, display sensitivity to large- x PDFs of the order 10 – 20% for $M_{W'} \gtrsim 2$ TeV at the LHC (due to \bar{d} and \bar{u}) and 0.75 TeV at the Tevatron (due again to d quarks). The uncertainties at central rapidity directly propagate to the integrated cross sections, which show $\lesssim 3\%$ effects for Z' production, while somewhat larger for W' production, amounting to $\lesssim 20\%$ for W'^+ and $\lesssim 10\%$ for W'^- at the LHC for $M_{W'} < 3$ TeV, and $\lesssim 30\%$ for W'^+ and W'^- at the Tevatron for $M_{W'} < 1$ TeV.

These considerations place important limits on the ability to accurately measure heavy W' and Z' cross sections in hadronic collisions, particularly at large rapidities and boson masses near the kinematic thresholds of current colliders. Although our analysis is, for illustration, restricted to heavy vector bosons with Standard Model couplings, and the quantitative effects of the PDF uncertainties would be different in other models, our main point is that caution must be exercised when using PDFs in regions where these are not directly constrained, or their uncertainties underestimated, as is the case at large x . The uncertainties in the production cross sections can be reduced by obtaining better constraints on PDFs at large x , especially for the d quark. Several experiments aimed at determining the d quark PDF up to $x \approx 0.8$ are planned at Jefferson Lab following its 12 GeV energy upgrade [21–23]. Uncertainties in cross sections at central rapidity, and hence in the integrated cross sections, will also be reduced with improved determinations of antiquark distributions at large x , such as the E-906/SeaQuest experiment at Fermilab [52] which plans to measure \bar{d}/\bar{u} up to $x \approx 0.45$.

The flavor dependence of weak boson production could also be studied with pn collisions at the LHC or at the Relativistic Heavy-Ion Collider, with the neutron provided by a beam of deuterons [53]. Unlike for fixed target experiments, in a collider one can study pd collisions at

large positive and negative rapidities. Therefore, partons in the beam at large x_1 can scatter from partons in the target at small x_2 , and vice versa. In particular, measurements at large negative rapidity would be sensitive to quarks in the deuteron at large momentum fractions, offering a probe of nuclear corrections complementary to deuterium DIS, and constraining the nuclear uncertainties studied in this paper.

Finally, while we have focussed on the $\sqrt{s} = 7$ TeV energy at which the LHC currently operates, in future this is planned to increase to $\sqrt{s} = 14$ TeV. The behavior of the cross sections illustrated here will not change qualitatively at the larger energy. However, for physical W and Z bosons, the region in rapidity where sensitivity to nuclear models is greatest will be shifted outside of the acceptance of current experiments, limiting the usefulness of 14 TeV data for large- x PDF studies. On the other hand, the higher center of mass energy will increase the accessible W', Z' mass range (up to $M_{W',Z'} \approx 6$ TeV) over a larger range of rapidities.

Acknowledgements

We thank D. del Re and J. Erler for helpful discussions and communications. This work was supported by the DOE contract No. DE-AC05-06OR23177, under which Jefferson Science Associates, LLC operates Jefferson Lab, DOE contract No. DE-FG02-97ER41022, DoD's ASSURE Program, and the National Science Foundation under NSF Contact Nos. 1062320 and 1002644.

-
- [1] S. Alekhin, J. Blümlein, P. Jimenez-Delgado, S. Moch and E. Reya, Phys. Lett. B **697**, 127 (2011); S. Alekhin, J. Blümlein and S. Moch, Eur. Phys. J. C **71**, 1723 (2011).
 - [2] R. S. Thorne and G. Watt, JHEP **1108**, 100 (2011).
 - [3] J. Baglio, A. Djouadi, S. Ferrag and R. M. Godbole, Phys. Lett. B **699**, 368 (2011); *Erratum* Phys. Lett. B **702**, 105 (2011); J. Baglio, A. Djouadi and R. M. Godbole, arXiv:1107.0281.
 - [4] A. Accardi *et al.*, Phys. Rev. D **81**, 034016 (2010).
 - [5] A. Accardi *et al.*, Phys. Rev. D **84**, 014008 (2011).
 - [6] S. Kuhlmann *et al.*, Phys. Lett. B **476**, 291 (2000).
 - [7] J. L. Hewett and T. G. Rizzo, Phys. Rep. **183**, 193 (1989).

- [8] A. Leike, Phys. Rep. **317**, 143 (1999).
- [9] T. G. Rizzo, in *Colliders and neutrinos*, Boulder, Colorado (2006), arXiv:hep-ph/0610104.
- [10] P. Langacker, Rev. Mod. Phys. **81**, 1199-1228 (2009).
- [11] S. A. Kulagin and R. Petti, Nucl. Phys. **A765**, 126 (2006).
- [12] Y. Kahn, W. Melnitchouk and S. A. Kulagin, Phys. Rev. C **79**, 035205 (2009).
- [13] W. Melnitchouk, A. W. Schreiber and A. W. Thomas, Phys. Rev. D **49**, 1183 (1994).
- [14] W. Melnitchouk, A. W. Schreiber and A. W. Thomas, Phys. Lett. B **335**, 11 (1994).
- [15] R. Machleidt, Phys. Rev. C **63**, 024001 (2001).
- [16] R. B. Wiringa, V. G. J. Stoks and R. Schiavilla, Phys. Rev. C **51**, 38 (1995).
- [17] F. Gross and A. Stadler, Phys. Rev. C **78**, 014005 (2008); *ibid.* C **82**, 034004 (2010).
- [18] M. Lacombe, B. Loiseau, R. Vinh Mau, J. Cote, P. Pires and R. de Tourreil, Phys. Lett. B **101**, 139 (1981).
- [19] O. Hen, A. Accardi, W. Melnitchouk and E. Piasetzky, Phys. Rev. D **84**, 117501 (2011).
- [20] J. Arrington, J. Rubin and W. Melnitchouk, arXiv:1110.3362 [hep-ph].
- [21] Jefferson Lab Experiment E12-10-102 [BoNuS12], S. Bültmann, M. E. Christy, H. Fenker, K. Griffioen, C. E. Keppel, S. Kuhn and W. Melnitchouk, spokespersons.
- [22] Jefferson Lab Experiment E12-10-103 [MARATHON], G. G. Petratos, J. Gomez, R. J. Holt and R. D. Ransome, spokespersons.
- [23] Jefferson Lab Experiment E12-10-007 [SoLID], P. Souder, spokesperson.
- [24] I. R. Afnan *et al.*, Phys. Lett. B **493**, 36 (2000);
I. R. Afnan *et al.*, Phys. Rev. C **68**, 035201 (2003).
- [25] E. L. Berger, F. Halzen, C. S. Kim and S. Willenbrock, Phys. Rev. D **40**, 83 (1989).
- [26] A. D. Martin, W. J. Stirling and R. G. Roberts, Phys. Rev. D **50**, 6734 (1994).
- [27] H. L. Lai *et al.*, Phys. Rev. D **51**, 4763 (1995).
- [28] W. Melnitchouk and J.-C. Peng, Phys. Lett. B **400**, 220 (1997).
- [29] S. Alekhin, J. Blumlein, S. Klein and S. Moch, Phys. Rev. D **81**, 014032 (2010).
- [30] H. L. Lai *et al.*, Phys. Rev. D **82**, 074024 (2010).
- [31] A. D. Martin, W. J. Stirling, R. S. Thorne and G. Watt, Eur. Phys. J. C **63**, 189 (2009).
- [32] R. D. Ball *et al.*, Nucl. Phys. **B849**, 112 (2011).
- [33] R. D. Ball *et al.*, Nucl. Phys. **B855**, 608 (2012).
- [34] V. Barger and R. Phillips, *Collider Physics*, Addison-Wesley (1987).

- [35] K. Nakamura *et al.*, J. Phys. G **37**, 075021 (2010).
- [36] T. Aaltonen *et al.* [CDF Collaboration], Phys. Rev. Lett. **102**, 181801 (2009).
- [37] V. M. Abazov *et al.* [D0 Collaboration], Phys. Rev. D **77**, 011106 (2008); V. M. Abazov *et al.*, Phys. Rev. Lett. **101**, 211801 (2008).
- [38] J. Campbell, K. Ellis and C. Williams, Phys. Rev. D **62**, 114012 (2000); *MCFM – Monte Carlo for FeMtobarn processes*, <http://mcfm.fnal.gov/>.
- [39] G. Aad *et al.* [ATLAS Collaboration], Phys. Lett. B **701**, 31 (2011).
- [40] S. Chatrchyan *et al.* [CMS Collaboration], JHEP **1104**, 050 (2011).
- [41] T. Shears [LHCb Collaboration], PoS EPS-HEP2009, 306 (2009).
- [42] A. Belloni and K. Lohwasser, *Comparison and combination of W lepton asymmetry from ATLAS, CMS and LHCb*, LHC Electroweak Working Group, preliminary report (2011).
- [43] J. L. Hewett and T. G. Rizzo, arXiv:hep-ph/9809525; H. K. Dreiner, P. Richardson and M. H. Seymour, Phys. Rev. D **63**, 055008 (2001); B. C. Allanach, M. Guchait and K. Sridhar, Phys. Lett. B **586**, 373 (2004).
- [44] I. Antoniadis, Phys. Lett. B **246**, 377 (1990); T. G. Rizzo and J. D. Wells, Phys. Rev. D **61**, 016007 (2000).
- [45] L. Randall and R. Sundrum, Phys. Rev. Lett. **83**, 3370 (1999).
- [46] T. Aaltonen *et al.* [CDF Collaboration], Phys. Rev. D **83**, 031102 (2011).
- [47] T. Aaltonen *et al.* [CDF Collaboration], Phys. Rev. Lett. **102**, 091805 (2009).
- [48] G. Aad *et al.* [ATLAS Collaboration], Phys. Lett. B **705**, 28 (2011).
- [49] G. Aad *et al.* [ATLAS Collaboration], Phys. Rev. Lett. **107**, 272002 (2011).
- [50] S. G. Porsev, K. Beloy and A. Derevianko, Phys. Rev. Lett. **102**, 181601 (2009).
- [51] J. Erler, P. Langacker, S. Munir and E. Rojas, JHEP **1111**, 076 (2011).
- [52] Fermilab Experiment E-906/SeaQuest, P. E. Reimer and D. Geesaman spokespersons.
- [53] C. Bourrely and J. Soffer, Nucl. Phys. **B423**, 329 (1994).